Monthly Notices of the ROYAL ASTRONOMICAL SOCIETY

MNRAS **530,** 1118–1128 (2024) https://doi.org/10.1093/mnras/stae883
Advance Access publication 2024 April 04

Generic gravito-magnetic clock effects

Kaye Jiale Li [1]★ Kinwah Wu [1]★ Ziri Younsi,[1]★ Joana Teixeira[1] and Dinesh Singh[2]

[1]*Mullard Space Science Laboratory, University College London, Holmbury St Mary, Surrey RH5 6NT, United Kingdom*
[2]*Department of Physics, University of Regina, Regina SK S4S 0A2, Canada*

Accepted 2024 March 25. Received 2024 March 13; in original form 2023 August 1

ABSTRACT

General relativity predicts that two counter-orbiting clocks around a spinning mass differ in the time required to complete the same orbit. The difference in these two values for the orbital period is generally referred to as the gravito-magnetic (GM) clock effect. It has been proposed to measure the GM clock effect using atomic clocks carried by satellites in prograde and retrograde orbits around the Earth. The precision and stability required for satellites to accurately perform this measurement remains a challenge for current instrumentation. One of the most accurate clocks in the Universe is a millisecond pulsar, which emits periodic radio pulses with high stability. Timing of the pulsed signals from millisecond pulsars has proven to be very successful in testing predictions of general relativity and the GM clock effect is potentially measurable in binary systems. In this work, we derive the generic GM clock effect by considering a slowly spinning binary system on an elliptical orbit, with both arbitrary mass ratio and arbitrary spin orientations. The spin–orbit interaction introduces a perturbation to the orbit, causing the orbital plane to precess and nutate. We identify several different contributions to the clock effects: the choice of spin supplementary condition and the observer-dependent definition of a full revolution and 'nearly identical' orbits. We discuss the impact of these subtle definitions on the formula for GM clock effects and show that most of the existing formulae in the literature can be recovered under appropriate assumptions.

Key words: black hole physics – gravitation – relativistic processes – celestial mechanics – time – pulsars: general.

1 INTRODUCTION

In Einstein's theory of general relativity a rotating mass distorts the space–time around it, leading to the precession of orbits of an object around this rotating mass. This is known as Lense–Thirring precession (Lense & Thirring 1918). It is a manifestation of frame dragging. An analogy to frame dragging can be found by comparing the phenomenon to electromagnetism, in which the gravitational mass is treated as equivalent to the electric charge and the gravitational field generated by a point mass is referred to as the gravito-electric field. The rotation of a point mass induces an additional gravitational field analogous to the magnetic field produced by a spinning charge in electromagnetism, and this additional gravitational field corresponds to the gravito-magnetic (GM) field. The gravito-electric field gives rise to a clock effect via gravitational time dilation (i.e. gravitational redshift), which has been widely applied in synchronizing clocks in Global Positioning System (GPS) satellites. Such time dilation was confirmed by Overstreet et al. (2022)[1] experimentally, using atomic interference.

The GM field also leads to desynchronization of the clocks for satellites moving in prograde and retrograde motion with respect to the Earth's rotation axis. Cohen, Rosenblum & Clifton (1988) obtained a 'synchronization gap' of 1.92×10^{-17} s for geosynchronous and antigeosynchronous orbits. Cohen & Mashhoon (1993) suggested another possible measurement of the GM clock effect, which arise from the difference in time periods between a full revolution of a prograde ($\mathcal{T}_+$) orbit and that of an otherwise equivalent retrograde ($\mathcal{T}_-$) orbit. This leads to the well-known formula

$$\mathcal{T}_+ - \mathcal{T}_- = 4\pi \frac{J}{M[c]^2} \,, \tag{1}$$

(see also e.g. Mashhoon, Gronwald & Theiss 1999; Tartaglia 2000; Iorio, Lichtenegger & Mashhoon 2002; Faruque 2004), where c is the speed of light, and J and M are respectively the spin angular momentum and mass of the Earth. This formula is applicable to circular orbits around the Earth, irrespective of whether they are geosynchronous or not. There are many interesting features of this time difference. The topological nature of this effect is evident from its independence on the orbit's radius, similar to the Aharonov–Bohm effect in quantum mechanics (Aharonov & Bohm 1959). This effect is expected to be about 10^{-7} s for the Earth (Cohen & Mashhoon 1993), well within the timing precision achieved by current atomic clocks (see Mann 2018). It has been proposed that two satellites orbiting the Earth in prograde and retrograde motion will be able to reveal this effect. However, the precise tracking of satellite positions, the dynamic part of Earth's gravity, and other factors such as radiation pressure pose significant challenges (see Gronwald et al. 1997; Lichtenegger, Gronwald & Mashhoon 2000).

★ E-mail: j-li.19@ucl.ac.uk (KJL); kinwah.wu@ucl.ac.uk (KW); z.younsi@ucl.ac.uk (ZY)

[1]We note that although the term 'gravitational Aharonov–Bohm effect' is used in their publication, it does not refer to the GM potential but to the gravito-electric potential.

A promising yet often overlooked approach to detect this effect is through binary pulsar systems. Millisecond pulsars are considered as the most stable natural clocks in our Universe. Their spin-down rates, $\mathrm{d}P/\mathrm{d}t$, are in general smaller than 10^{-16} s s^{-1}, which corresponds to a drift of a few seconds over the Hubble time (see e.g. Lorimer 2008; Manchester 2017). The rotational stability of millisecond pulsars makes them a useful apparatus to measure the relativistic effects that are intrinsically small. For instance, the accurate measurement of the rate of decrease in the orbital period of the Hulse–Taylor binary provided the first indirect proof of emission of gravitational radiation (see Taylor & Weisberg 1989; Weisberg & Taylor 2005). The various gravitational time dilation effects have been widely used in analysing the pulsar timing data (see e.g. Edwards, Hobbs & Manchester 2006; Lorimer & Kramer 2012). Pulsars can also be used to test the equivalence principle (see Stairs 2003, for a review). For example the triple stellar system PSR J0337+1715 has provided a constraint on the strong-field violation of strong equivalence principle (Shao 2016; Archibald et al. 2018; Voisin et al. 2020). Similarly, Remmen & Wu (2013) proposed testing general relativity with a hierarchical three-body system consisting of a double-pulsar system revolving around a massive black hole. It was also demonstrated that extreme-mass-ratio binaries with a fast-spinning pulsar revolving around a massive black hole can be used as a probe of the relativistic spin–orbit coupling (see Singh, Wu & Sarty 2014; Kimpson, Wu & Zane 2019; Li, Wu & Singh 2019; Kimpson, Wu & Zane 2020; Li et al. 2022; Wu 2022).

In order to measure the GM clock effects in a pulsar binary system, it is necessary to derive the formula of the clock effect for a generic orbit. Previous studies (Cohen & Mashhoon 1993; Mashhoon et al. 1999; Tartaglia 2000; Bini, Jantzen & Mashhoon 2001, 2002; Iorio et al. 2002; Faruque 2004) mostly focused on circular orbits with spin aligned or anti-aligned with the orbital angular momentum, such that the orbits remain on the equatorial plane. Teyssandier (1977, 1978) extended the study to orbits around a rotating non-spherical mass. Faruque, Ahsan & Ishwar (2003) derived a different GM clock effect formula by comparing the prograde innermost stable circular orbit and the retrograde innermost stable circular orbit. The effect of the cosmological constant on the GM clock effect is studied by Kerr, Hauck & Mashhoon (2003). Mashhoon et al. (1999) and Iorio et al. (2002) generalized the GM clock effect to arbitrary inclination angle for circular orbits. As well, Mashhoon, Iorio & Lichtenegger (2001) extended their work to eccentric and inclined orbits in an Earth-satellite system, under the exact GM analogue. The effect of eccentricity is also taken into account by Hackmann & Lämmerzahl (2014) by studying the motion of test particles in Kerr space–time on eccentric orbits. They obtained results that differ from those of other literature on the topic. The effect of spin for the test mass on circular (or semicircular) orbits is included by Bini, de Felice & Geralico (2004a,b), Faruque (2006), and Mashhoon & Singh (2006) but different coefficients were reported.

In this work, we derive a formula for the general GM clock effect involving two spinning masses on an orbit with arbitrary inclination and eccentricity. The formula is applicable over a large parameter range, and we show that it can reproduce the results obtained in most other previous studies with appropriate assumptions. We also clarify the origin of apparent discrepancy in the formulae reported in different papers. We organize the paper as follow. Section 2 gives a brief introduction to spin–orbit coupling with different spin supplementary conditions (SSCs). Section 3 presents the equations of motion (EOM) of a binary system subjected to the spin–orbit coupling force and our derivation of the generic formula for GM clock effect. We show in Section 4 our results are generalization of many previous works and how we may use our formula to resolve the issues of the discrepancies of previous work. We also provide an in-depth exposition of the concept of GM clock effects, highlighting common misconceptions and misinterpretations (of results in observations) often found in literature. Further, we comment on implications on the observation of the GM clock effect via the pulsar binary, and via artificial satellite systems. Unless otherwise stated, we adopt the [$-,+,+,+$] metric signature convention and the natural unit system with $c = G = 1$ in this paper, where c is the speed of light and G is the gravitational constant.

2 SPIN–ORBIT COUPLING

2.1 Spin–orbit coupling and spin supplementary condition

Consider a binary system with masses m_1 and m_2, respectively located at $\boldsymbol{r}_1$ and $\boldsymbol{r}_2$, moving with $\boldsymbol{v}_1$ and $\boldsymbol{v}_2$ with respect to their centre-of-mass. We define a mass ratio $q \equiv m_2/m_1$. The total mass of the binary is therefore $M = m_1 + m_2 = m_1(1+q)$, the relative position $\boldsymbol{r} = \boldsymbol{r}_1 - \boldsymbol{r}_2$ and relative velocity $\boldsymbol{v} = \boldsymbol{v}_1 - \boldsymbol{v}_2$. It follows that the total spin $\boldsymbol{S} = \boldsymbol{S}_1 + \boldsymbol{S}_2$, and the mass−weighted total spin is $\boldsymbol{\sigma} = q\,\boldsymbol{S}_1 + q^{-1}\boldsymbol{S}_2$. As the GM clock effect can only be measured in a system with at least one accurate clock, we take m_1 to be a pulsar (neutron star) and m_2 be its companion star. There are no restrictions on the value of q in the derivation presented in this work, i.e. the companion star can be less or more massive than the pulsar, and hence it can a main-sequence star, a white dwarf, a neutron star or a black hole.

In additional to the Newtonian gravitational force $-M\boldsymbol{r}/r^3$, the spin–orbit coupling force produces an additional acceleration on the binary, and it is given by

$$\boldsymbol{a}_{\rm SO} = \frac{1}{r^3}\left\{\frac{3}{r^2}\boldsymbol{r}\left[(\boldsymbol{r}\times\boldsymbol{v})\cdot((k+1)\,\boldsymbol{\sigma}+2\boldsymbol{S})\right] + \frac{3\dot{r}}{r}\left[\boldsymbol{r}\times((2-k)\boldsymbol{\sigma}+2\boldsymbol{S})\right] - \boldsymbol{v}\times(3\boldsymbol{\sigma}+4\boldsymbol{S})\right\} \tag{2}$$

(Kidder 1995), with k a parameter depending on the chosen spin supplementary condition (SSC). Here and hereafter, 'dot' above a variable represents the differentiation with respect to time. It is worth noting that the SSC only affects the coefficient of $\boldsymbol{\sigma}$. Before delving into the discussion of SSC, it is important to highlight that there exists a gravito-electric effect [i.e. the 1pN (post-Newtonian) effect], which is typically more significant than the spin–orbit coupling effect (a 1.5pN effect). However, the gravito-electric effect does not contribute to $\mathcal{T}_+ - \mathcal{T}_-$ (see equation 21 of Wu 2022). It is also crucial to emphasize that the GM clock effect is inherently topological, as evidenced by the absence of orbital size in the formula equation (1). While higher order spin contributions, such as the interplay of the gravito-electric effect with the GM effect (first appearing at 2.5pN order) and spin–spin coupling (appearing at the 2pN order), do influence the precession speed difference between retrograde and prograde orbits, they do not qualify as part of the GM clock effect. Therefore, we do not include the contributions of these higher order effects in this work.

The SSC and, hence, the coefficient k depend on the definition of the centre-of-mass. For a spinning sphere of mass m and spin magnitude s, the centre-of-mass depends on the observer (see e.g. Costa et al. 2012). For an observer co-moving with the spinning sphere, the centre-of-mass coincides with its geometrical centre. While for an observer moving with $\boldsymbol{v}$ with respect to the sphere, the centre-of-mass is displaced by $\boldsymbol{v}\times\boldsymbol{s}/m$. The set of centres-of-

mass determined by all possible observers form a disc perpendicular to the spin axis with a radius of s/m, which is called the Möller radius.

In principle, any observer can be chosen to describe the motion of the spinning object, although some choices are more natural than others. In the literature, there are a few conventional choices which give rise to different values for k: the Frenkel–Mathisson–Pirani condition (Frenkel 1926; Mathisson 1937), which is also equivalent to the Tulczyjew–Dixon (Tulczyjew 1959; Dixon 1964) condition at linear order in spin, corresponds to the case of $k = 1$. At linear order in spin, these two conditions both correspond to adopting an observer co-moving with the spinning particle. The Newton–Wigner–Pryce condition (Pryce 1948; Newton & Wigner 1949) is associated with $k = 1/2$. Although the physical interpretation of this condition remains unclear, it has certain advantages. For instance, it is the only SSC that leads to vanishing Poisson brackets in both flat space–time (Pryce 1948; Newton & Wigner 1949; Hanson & Regge 1974) and curved space–time (Barausse, Racine & Buonanno 2009). The Corinaldesi–Papapetrou condition (Corinaldesi & Papapetrou 1951), which is equivalent to adopting a set of static observers, corresponds to $k = 0$.

The general-relativistic representation of these SSCs for a spinning particle with 4-momentum p^μ and spin tensor $S^{\mu\nu}$ may be written as follows:

$$S^{\mu\nu}u_\nu = 0 \text{ or } S^{\mu\nu}p_\nu = 0 \Rightarrow k = 1, \tag{3a}$$

$$S^{\mu\nu}(p_\nu - me^{\hat{0}}{}_\nu) = 0 \Rightarrow k = \frac{1}{2}, \tag{3b}$$

$$S^{0\nu} = 0 \Rightarrow k = 0. \tag{3c}$$

Here, $m \equiv \sqrt{-p^\mu p_\mu}$ is the dynamical mass and u^μ is the 4-velocity of the centre-of-mass of the spinning particle. The tensor $e^{\hat{a}}{}_\nu$ represents the natural tetrad field satisfying

$$e^{\hat{a}}{}_\mu e^{\hat{b}}{}_\nu g^{\mu\nu} = \eta^{\hat{a}\hat{b}}, \tag{4}$$

where $\eta^{\hat{a}\hat{b}} = \mathrm{diag}(-1, 1, 1, 1)$. The tensor field $e^{\hat{0}\nu}$ is time-like and past-oriented, such that $e^{\hat{0}}{}_0 > 0$.

3 PERTURBATION TO NEWTONIAN ORBITS

3.1 Perturbation to the orbit

In this section, we follow the method in Mashhoon et al. (2001) to calculate the orbital perturbation due to the spin–orbit couplings for a binary system. In the absence of spin, the binary's motion follows a Newtonian orbit confined to the plane perpendicular to the orbital angular momentum. We refer to the orbit of a non-spinning binary as the *unperturbed* orbit and the orbit of a slowly spinning binary as the *perturbed* orbit. Let us first consider the Cartesian coordinates (x, y, z) with $\hat{\boldsymbol{z}}$ parallel to the unperturbed orbital angular momentum. The total spin $\boldsymbol{S}$ has polar angle θ_S and azimuthal angle ϕ_S with respect to the (x, y, z) coordinate. Similarly, the mass–weighted spin has polar angle θ_σ and azimuthal angle ϕ_σ. The geometry of the binary system in shown in Fig. 1.

It is convenient to adopt cylindrical coordinates (ρ, ϕ, z) for the orbit, with the $\hat{z}$-axis parallel to the (unperturbed) orbital angular momentum. In the following, the subscript '0' denotes the unperturbed Newtonian orbit. We have $z_0 = 0$ for the unperturbed orbit. The other two coordinates are given by:

$$\rho_0 = \frac{a_0(1 - e_0^2)}{e_0 \cos v_0 + 1}, \tag{5a}$$

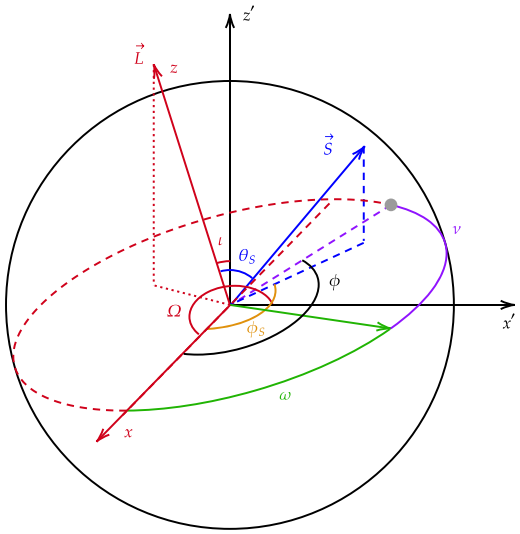

Figure 1. An illustration of the geometrical configuration of the system. The unperturbed orbit is located on the $z = 0$ plane in (x, y, z) coordinates, with its angular momentum in the $\hat{\boldsymbol{z}}$ direction. ω is the argument of periapsis. ϕ is the azimuthal angle with respect to $\hat{\boldsymbol{x}}$ and $v \equiv \phi - \omega$ is the true anomaly. The observer is located on the $x' - y'$ plane. ι and Ω are the inclination angle and longitude of ascending node, respectively, with respect to $x' - y'$ plane. The dashed lines represent lines on and projections on to the $x - y$ plane. The dotted lines represent projections on to the $x' - y'$ plane. The polar angle θ_S and azimuthal angle ϕ_S of the total spin vector are defined with respect to the (x, y, z) coordinate. The mass–weighted spin vector, which is similarly defined, is omitted from the figure.

$$\phi_0 = \omega_0 + 2\arctan\left[\sqrt{\frac{1 + e_0}{1 - e_0}}\tan\frac{E_0}{2}\right], \tag{5b}$$

where a_0 and e_0 are the (unperturbed) semimajor axis and eccentricity, $v_0 \equiv \phi_0 - \omega_0$ is the true anomaly, and E_0 is the eccentric anomaly, which is related to the orbital period P_0 via $E_0 - e_0 \sin E_0 = 2\pi/P_0$. For a Newtonian orbit, $P_0 = 2\pi\sqrt{a_0{}^3/M}$. The angular momentum of the unperturbed orbit per reduced mass is $L_0 \equiv \sqrt{Ma_0(1 - e_0^2)}$.

Cylindrical coordinates are related to Cartesian coordinates via $(x, y, z) \equiv (\rho\cos\phi, \rho\sin\phi, z)$. We may therefore write the spins $\boldsymbol{\sigma}$ and $\boldsymbol{S}$ in cylindrical coordinates, thereby decomposing the acceleration due to the spin–orbit coupling force into the three directions:

$$\boldsymbol{a}_{\mathrm{SO}} = C_\rho\frac{\dot{\phi}}{\rho^2}\hat{\boldsymbol{\rho}} + C_\phi\frac{\dot{\rho}}{\rho^3}\hat{\boldsymbol{\phi}} + \left(C_{z,\phi}\frac{\dot{\phi}}{\rho^2} + C_{z,\rho}\frac{\dot{\rho}}{\rho^3}\right)\hat{\boldsymbol{z}}, \tag{6}$$

where

$$C_\rho = 3k\sigma\cos\theta_\sigma + 2S\cos\theta_S, \tag{7a}$$

$$C_\phi = 3(k-1)\sigma\cos\theta_\sigma - 2S\cos\theta_S, \tag{7b}$$

$$C_{z,\phi} = 3\sigma\sin\theta_\sigma\cos(\phi - \phi_\sigma) + 4S\sin\theta_S\cos(\phi - \phi_S), \tag{7c}$$

$$C_{z,\rho} = 3(k-1)\sigma\sin\theta_\sigma\sin(\phi - \phi_\sigma) - 2S\sin\theta_S\sin(\phi - \phi_S). \tag{7d}$$

Therefore, the EOMs of the binary under the perturbation is given by

$$\ddot{\rho} - \rho\dot{\phi}^2 + \frac{M}{\rho^2} = C_\rho\frac{\dot{\phi}}{\rho^2}, \tag{8a}$$

$$\rho\ddot{\phi} + 2\dot{\rho}\dot{\phi} = C_\phi\frac{\dot{\rho}}{\rho^3}, \tag{8b}$$

$$\ddot{z} + \frac{M}{\rho^3} z = C_{z,\phi} \frac{\dot{\phi}}{\rho^2} + \epsilon\, C_{z,\rho} \frac{\dot{\rho}}{\rho^3} \,. \tag{8c}$$

We have introduced a new factor, $\epsilon \equiv |\boldsymbol{a}_{\rm SO}|/|\boldsymbol{a}_{\rm N}|$, to quantify the magnitude of the spin–orbit coupling force relative to the Newtonian gravitational force. The expressions on the right-hand sides of the equations (8a–c) are of order $\sim \mathcal{O}(\epsilon)$. Since we are primarily interested in the GM clock effect under the assumption of slow rotation, we retain only the terms up to first order in the perturbation due to the spin–orbit coupling force. Consequently, all terms of order $\mathcal{O}(\epsilon^2)$ or higher are ignored. Equation (8b) can also be rewritten as

$$\frac{\mathrm{d}(\rho^2\dot{\phi})}{\mathrm{d}\,t} = \frac{C_\phi \dot{\rho}}{\rho^2} \,, \tag{9}$$

whose solution is simply

$$\rho^2\dot{\phi} = C_1 - \frac{C_\phi}{\rho} \,, \tag{10}$$

where C_1 is some constant which should reduce to the angular momentum L_0 when both spins vanish. Therefore, we have $C_1 - L_0 \sim \mathcal{O}(\epsilon)$, $\rho - \rho_0 \sim \mathcal{O}(\epsilon)$, and similarly for ϕ and z.

Using the formula for $\dot{\phi}$ in equation (10), and defining $u \equiv 1/\rho$, equation (8a) can be rewritten, with the help of equation (5a), as a second order differential equation for u:

$$\begin{aligned}\frac{\mathrm{d}^2u}{\mathrm{d}\phi^2} + u = \frac{M}{C_1^2} + \frac{\left(1-e_0^2\right)^{-2}}{a_0^2 C_1}\{C_\phi \left[1 - e_0^2\cos\left(2\phi_0 - 2\omega_0\right)\right] \\ + \left(C_\phi - C_\rho\right)\left[e_0\cos\left(\phi_0 - \omega_0\right) + 1\right]^2\} \,,\end{aligned} \tag{11}$$

where C_1 remains undetermined. The second term on the right-hand side of equation (11) corresponds to a linear-order correction in ϵ. Consequently, we may introduce a quantity similar to the semimajor axis, denoted by $a = a_0(1+\alpha)$ where $\alpha \sim \mathcal{O}(\epsilon)$, and a quantity similar to eccentricity, denoted by $e = e_0(1+\eta)$ where $\eta \sim \mathcal{O}(\epsilon)$. We can use these definitions interchangeably with a_0 and e_0 as per convenience, and this substitution would only contribute to the perturbation at the second order in ϵ^2. We can also replace C_1 with L_0 using the same reasoning.

Combining this differential equation and form of unperturbed orbit, we can guess the solution to be of the form

$$u = \frac{1 + e\cos[(1+C_3)\phi - \omega] + C_2\cos[2(1+C_3)\phi - 2\omega]}{a(1-e^2)} \,, \tag{12}$$

where $\omega \equiv \omega_0 + \xi$. It is important to note that these definitions do not necessarily represent the semimajor axis, eccentricity, and argument of periapsis of the perturbed orbit. However, these definitions correspond to those of the unperturbed orbit when both spins vanish. In the solution, we have $C_1 - L_0 \sim \mathcal{O}(\epsilon)$. C_2, C_3, α, η, and ξ are all small corrections of linear order in ϵ. Among these, C_3 represents the orbital precession due to the spin–orbit coupling force, while C_2 represents the non-sinusoidal variation of the orbit. There are five unknowns (a, e, ξ, C_2, and C_3) in this solution, and one unknown C_1 in the differential equation. Next, we perform a Taylor expansion of the proposed solution with respect to ϵ and compare it with the differential equation, disregarding terms of order $\mathcal{O}(\epsilon^2)$. The constant term in u, and the coefficients of $\phi\sin(\phi - \omega_0)$ and $\cos(2\phi - 2\omega_0)$ inside the Taylor expansion of u would be used to eliminate three degrees of freedom, leaving α, η, and ξ as the free variables. It follows that

$$C_2 = \frac{e_0^2 M}{6L_0^3}(C_\rho + C_\phi) \,, \tag{13}$$

$$C_3 = \frac{M}{L_0^3}(C_\rho - C_\phi) \,, \tag{14}$$

$$\begin{aligned}C_1 = L_0 - \frac{M}{4L_0^2}\{2a_0L_0[e_0^2(\alpha + 2\eta) - \alpha] \\ + (e_0^2+2)C_\rho - (e_0^2+4)C_\phi\} \,.\end{aligned} \tag{15}$$

The remaining free variables can be determined by the value of u, $\dot{u}$ and $\dot{\phi}$ at a given time instance (or at three different time instances).

It is worth noting that C_1 can also be expressed as a function of a and e:

$$C_1 = \sqrt{Ma(1-e^2)} + \frac{1}{4a\left(1-e^2\right)}\left[\left(e^2+4\right)C_\phi - \left(e^2+2\right)C_\rho\right] \,. \tag{16}$$

The motion in the z-direction can be solved by assuming $z = \rho H(\phi)$ (Mashhoon 1978; Mashhoon et al. 2001), where $H(\phi)$, as well as its derivatives, are of linear order in ϵ. Ignoring second order perturbations, and applying equations (8a–c), we obtain a differential equation for z:

$$\rho\dot{\phi}^2\left(\frac{\mathrm{d}^2H}{\mathrm{d}\phi^2} + H\right) = C_{z,\phi}\frac{\dot{\phi}}{\rho^2} + C_{z,\rho}\frac{\dot{\rho}}{\rho^3} \,. \tag{17}$$

(Note that both sides of the equation are linear in ϵ.) Replacing ρ, $\dot{\phi}$, and $\dot{\rho}$ with $1/u$, $(C_1u^2 - \epsilon C_\phi u^3)$, and $-\dot{u}/u^2$, respectively, and upon ignoring terms above first order, the differential equation for $H(\phi)$ may be rewritten as

$$\frac{\mathrm{d}^2H}{\mathrm{d}\phi^2} + H = \frac{M}{L_0^3}\{e_0C_{z,\rho}\sin(\phi - \omega_0) + C_{z,\phi}[e_0\cos(\phi - \omega_0) + 1]\} \,. \tag{18}$$

The general solution of $H(\phi)$ that is accurate to linear order in ϵ is

$$\begin{aligned}H = \frac{M}{4L_0^3}\{\phi[6\sigma\sin\theta_\sigma\sin(\phi - \phi_\sigma) + 8S\sin\theta_S\sin(\phi - \phi_S)] \\ + C_4\sin\phi + C_5\cos\phi + 2e_0[\sigma\sin\theta_\sigma(3k\cos(\phi_\sigma - \omega_0) \\ + (k-2)\cos(2\phi - \phi_\sigma - \omega_0)) \\ + 4S\sin\theta_S\sin(\phi - \phi_S)\sin(\phi - \omega_0)]\} \,,\end{aligned} \tag{19}$$

with C_4 and C_5 being arbitrary constants which are linear in ϵ. These two degrees of freedom can be determined by the value of z and $\dot{z}$ at a given time instance (or two different instances). Further, it is notable that H grows secularly as $\phi \to \infty$, emphasizing that the formula will be less accurate as the number of orbit increases.

3.2 Projection of orbit on the observer's coordinate system

We adopt a new Cartesian coordinate system (x', y', z') for the observer (i.e. a terrestrial radio telescope in case of pulsar timing or a laser ranging site for artificial satellite) with the observer placed on the $x' - y'$ plane. We note that the definition of inclination angle here is different from the convention adopted in binary system observations, and an edge-on orbit corresponds to $\iota = 0$ in our definition. To simplify calculations, we may ignore the relative motion between the centre-of-mass of the binary and the observer, such that both coordinate systems (x, y, z) and (x', y', z') remain static. These coordinate systems are related via the rotation

$$\begin{bmatrix} x' \\ y' \\ z' \end{bmatrix} = \begin{bmatrix} \cos\Omega & -\cos\iota\sin\Omega & \sin\iota\sin\Omega \\ \sin\Omega & \cos\iota\cos\Omega & -\cos\Omega\sin\iota \\ 0 & \sin\iota & \cos\iota \end{bmatrix} \begin{bmatrix} x \\ y \\ z \end{bmatrix} \,, \tag{20}$$

where Ω is the longitude of the ascending node and ι is the inclination angle with respect to the reference plane $x' - y'$. We also introduce the spherical coordinate system (R, φ, ϑ), which is defined with respect to (x', y', z').

3.3 General solution

Because a_0, e_0, and ω_0 are all parameters that are not directly measurable, the results are instead expressed in terms of a, e, and ω. This choice of variables eliminates the three degrees of freedom represented by α, η, and ξ. Due to precession, the orbit is no long closed (expect for when the orbit is strictly circular, even under perturbations). To account for this, we introduce an additional term ϕ_1, of linear order in ϵ, which characterises the nutation and precession of the orbital plane. Assuming a full orbit starts at $\phi = \phi_0$ and ends at $\phi = \phi_0 + 2\pi + \epsilon\phi_1$, the time it takes to complete a full orbit is:

$$\begin{aligned}\mathcal{T} &= \int_{\phi_0}^{\phi_0+2\pi+\epsilon\phi_1} \frac{\mathrm{d}\phi}{C_1 u^2 - \epsilon C_\phi u^3} \\ &= 2\pi\sqrt{\frac{a^3}{M}} + \frac{\pi}{2(1-e^2)^{5/2}M} \\ &\quad \times \left[(-3e^4+3e^2-2)C_\rho + (3e^4-9e^2+4)C_\phi\right] \\ &\quad + \frac{1}{M\left[1+e\cos(\omega-\phi_0)\right]^2} \\ &\quad \times \left[2\pi\left(C_\rho - C_\phi\right) + a^{3/2}(1-e^2)^{3/2}\sqrt{M}\,\phi_1\right] . \end{aligned} \tag{21}$$

The angle ϕ_1 depends on the definition of a full orbit. To linear order in ϵ, the period difference between the perturbed and unperturbed orbit is given by:

$$\Delta\mathcal{T} = \mathcal{T} - 2\pi\sqrt{\frac{a_0^3}{M}} = \Delta\mathcal{T}_{\rm size} + \Delta\mathcal{T}_{\rm fixed} + \Delta\mathcal{T}_{\rm orb} , \tag{22}$$

where

$$\Delta\mathcal{T}_{\rm size} = 2\pi\sqrt{\frac{a^3}{M}} - 2\pi\sqrt{\frac{a_0^3}{M}} = 3\pi\alpha\sqrt{\frac{a_0^3}{M}} , \tag{23a}$$

$$\Delta\mathcal{T}_{\rm fixed} = \frac{\pi\left[(-3e^4+3e^2-2)C_\rho + (3e^4-9e^2+4)C_\phi\right]}{2(1-e^2)^{5/2}M} , \tag{23b}$$

$$\Delta\mathcal{T}_{\rm orb} = \frac{\left[a^{3/2}(1-e^2)^{3/2}\sqrt{M}\phi_1 + 2\pi\left(C_\rho - C_\phi\right)\right]}{M\left[1+e\cos(\omega-\phi_0)\right]^2} . \tag{23c}$$

To linear order in ϵ, replacing e with e_0 does not affect the three terms, hence they are independent of the free parameter η. $\Delta\mathcal{T}_{\rm fixed}$ is independent of the choice of α, ϕ_1 or ϕ_0. $\Delta\mathcal{T}_{\rm size}$ depends on the free parameter α, and therefore represents the period difference due to the difference in size of the perturbed and unperturbed orbits. As we will discuss later, this difference is related to the non-unique definition of 'nearly identical' orbits. $\Delta\mathcal{T}_{\rm orb}$ depends on the definition of a full revolution and on the initial position ϕ_0. Because α and ϕ_1 are free parameters (as long as they are linear in ϵ), $\Delta\mathcal{T}_{\rm fixed}$ and $\Delta\mathcal{T}_{\rm orb}$ are somewhat arbitrary and can themselves vanish, or be fine-tuned to make $\Delta\mathcal{T}$ vanish under suitable parameter choices.

This is part of the reason why the GM clock effect formula differs across the literature. These differences will be discussed in further detail in the following section. To clarify, the GM clock difference usually refers to the period difference between a prograde orbit and a retrograde orbit. In our case, we define $\Delta\mathcal{T}$ as the difference in period between a spinning and non-spinning binary system, which is about half of the GM clock effect commonly referred to in the literature.

3.4 A full revolution: $\Delta\mathcal{T}_{\rm orb}$

Consider an observer at $(R, \varphi, \vartheta) = (\infty, \varphi_0, \pi/2)$ and a binary approximately edge-on (such that $\iota \ll \pi/2$). A full orbit can be defined as the orbit with φ moving from φ_0 (which corresponds to $\phi = \phi_0$) to $\varphi_0 + 2\pi$ (which corresponds to $\phi = \phi_0 + 2\pi + \epsilon\phi_1$), with φ defined as:

$$\tan\varphi \equiv \frac{y'}{x'} = \frac{\sin\Omega\cos\phi + \cos\Omega\cos\iota\sin\phi - \epsilon H(\phi)\cos\Omega\sin\iota}{\cos\Omega\cos\phi - \sin\Omega\cos\iota\sin\phi + \epsilon H(\phi)\sin\Omega\sin\iota} . \tag{24}$$

Such an azimuthal closure would correspond to two sequential pulsar superior conjunctions (or approximately, two maximum Shapiro delays) for this observer. The duration of such an orbit is known as the sidereal period, as shown in the top panel of Fig. 2. With this definition, the angle ϕ_1 can be calculated by solving $\tan\varphi|_{\phi=\phi_0} = \tan\varphi|_{\phi=\phi_0+2\pi+\epsilon\phi_1}$, yielding:

$$\begin{aligned}\phi_1 = &-\frac{\pi M}{{L_0}^3}\tan\iota\cos\phi_0 \\ &\times\left[\,3\sigma\sin\theta_\sigma\sin(\phi_\sigma-\phi_0) + 4S\sin\theta_S\sin(\phi_S-\phi_0)\right] . \end{aligned} \tag{25}$$

This formula is independent of the SSC condition as it roots from the $\boldsymbol{v}\times(3\boldsymbol{\sigma}+4\boldsymbol{S})$ part of the spin–orbit coupling force, from which the parameter k is absent. When the inclination angle is zero, the $x - y$ plane overlaps with the $x' - y'$ plane and we have $\phi_1 = 0$, as expected.

There are other possible definitions of a full orbit. Considering an observer on the $x' - y'$ plane, the azimuthal closure is well-defined for nearly edge-on orbits, but it loses its meaning for face-on orbits. A more sensible definition of a full revolution for eccentric face-on orbits can be defined by the time interval between two successive periapsis passages, which is also known as the anomalistic period, as shown in the middle panel of Fig. 2. This definition corresponds to the time difference between two sequential maxima of the Einstein time delay. Under this assumption, the full orbit is defined as $\mathrm{d}u/\mathrm{d}\phi|_{\phi=\phi_0} = \mathrm{d}u/\mathrm{d}\phi|_{\phi=\phi_0+2\pi+\epsilon\phi_1} = 0$. Both the initial position ϕ_0, and ϕ_1, are independent of the observer's location. The expression for ϕ_1 is given by:

$$\phi_1 = \frac{2\pi M}{{L_0}^3}\left(C_\phi - C_\rho\right) . \tag{26}$$

That this definition of a full revolution yields $\Delta\mathcal{T}_{\rm orb} = 0$ is expected. Although this expression is not divergent as $e_0 \to 0$, it is important to emphasize that it is not applicable to circular orbits. In the limit of a circular orbit, the physical meaning of the anomalistic period becomes invalid due to the absence of periapsides. The bottom panel of Fig. 2 demonstrates the nodal period (or draconic period). It is defined as the time interval between two successive upward crossings of the $x' - y'$ plane. These crossing points are known as the ascending nodes, which correspond to the vanishing of

$$z' = \epsilon\rho H(\phi)\cos\iota + \rho\sin\iota\sin\phi . \tag{27}$$

For simplicity, we set $H(0) = 0$ such that the first ascending node corresponds to $\phi = 0$. The second passage can be found by solving $z'|_{\phi=2\pi+\epsilon\phi_1} = 0$. To linear order in ϵ, one finds:

$$\phi_1 = \frac{\pi M}{{L_0}^3}\cot\iota\left(3\sigma\sin\phi_\sigma\sin\theta_\sigma + 4S\sin\phi_S\sin\theta_S\right) . \tag{28}$$

As expected, the nodal period diverges when $\iota \to 0$, since the ascending node is not well-defined in this case. When $\iota = \pi/2$ we have $\phi_1 = 0$.

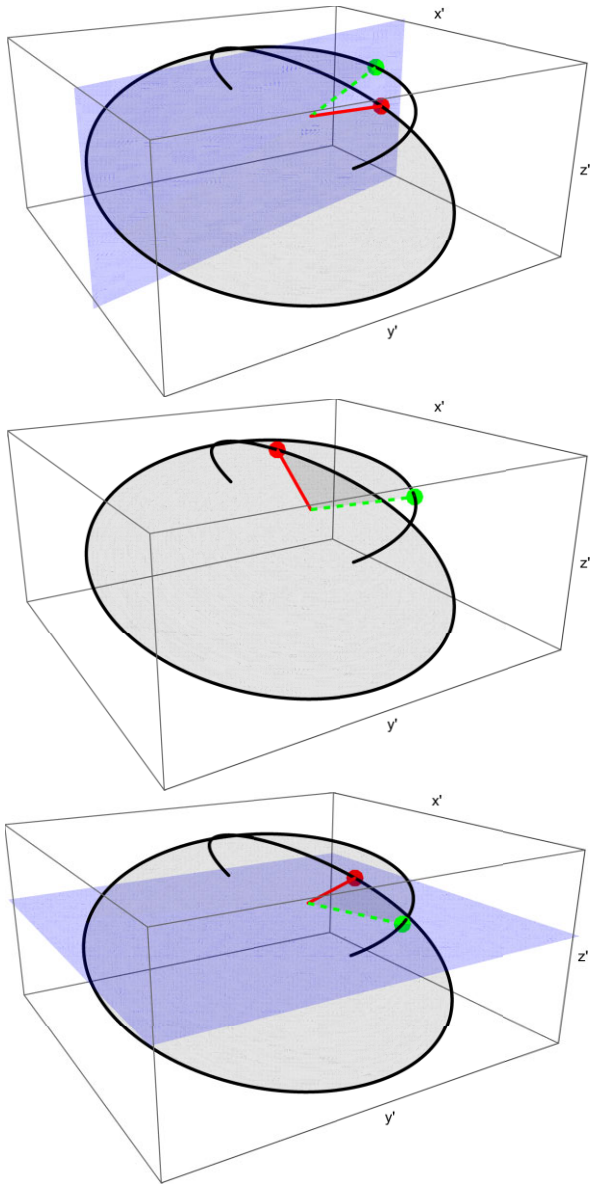

Figure 2. These figures illustrate different ways of defining a full orbital period. The top panel shows the sidereal period defined with respect to a distant observer on the vertical plane. The middle panel shows the anomalistic period, which is independent of observer's position. The bottom panel displays the nodal period, which is the duration between two successive upward crossings of the $z' = 0$ plane. In each panel, the curved solid line represents the perturbed orbit, with the perturbing force exaggerated for clarity. The dot connected to the origin with dashed (solid) line marks the start (end) point of the specific orbital period. The sector that the orbit sweeps through during one orbital period is shaded.

The above definitions are not unique. For example the synodic period, which is defined with reference to two or more observers (e.g. the Earth and the Sun) would be a more feasible definition for the measurement of the GM clock effect with artificial satellites. Most importantly, all of these different definitions of orbital period are identical for a binary under Newtonian gravity in the absence of any perturbing force, but differ for perturbed orbits.

3.5 Nearly-identical orbits: $\Delta\mathcal{T}_{\rm size}$

The GM clock effect is usually represented by the difference in the orbital period of a prograde (i.e. $\boldsymbol{S}\cdot\boldsymbol{L} > 0$) orbit and that of an identical retrograde (i.e. $\boldsymbol{S}\cdot\boldsymbol{L} < 0$) motion. However, from a theoretical perspective, there are no identical orbits when the spin–orbit force is included. This is simple to illustrate: the radial motion, i.e. equation (12), has additional terms with approximately two times the orbital frequency (i.e. the term with coefficient C_2) and a precession term, C_3. While it is possible to fix both C_2 and C_3 to vanish simultaneously, the motion in the z-direction cannot also be fixed to vanish, and vice versa. Even for circular orbits which seem very much similar, the angular velocity for orbits with identical radii will be different. This difference in angular velocity is in fact the source of the GM clock effect.

Therefore, before proceeding to calculate the GM clock effect, the orbits that we choose to compare must be carefully specified. We will refer to these orbits as 'nearly identical' or indistinguishable orbits. The non-unique choice of what constitutes two 'nearly identical' orbits can be translated into the choice of the free variable α, which is somewhat arbitrary and can be fine-tuned to make the time difference vanish. For example if we define two 'nearly identical' circular orbits as two circular orbits with the same $\dot{\phi}$ but slightly different radii (at the $\sim \mathcal{O}(\epsilon)$ level), the clock effect for a full revolution will vanish for these two nearly identical orbits.

The definition of 'nearly identical' is best clarified in terms of observable parameters. For pulsar observations, the main observables are the time delay due to pulse-arrival-time and Doppler effects. In general, it would be natural to define nearly identical orbits as those that result in indistinguishable observational signatures. For example if two different orbits can be fitted by the same template with exactly the same parameters, these two orbits will be considered nearly identical. However, such a definition can be quite subtle, and is dependent on the observation carried out, the noise level, and the template used to fit the data.

In the simplified model where the centre-of-mass of the binary is at rest with respect to the observer, there are several sources of time delays, in particular: (i) the Roemer delay due to the displacement of the pulsar relative to the centre-of-mass, (ii) the Shapiro delay due to the passage of light ray around the companion, and (iii) the Einstein delay due to time dilation in the gravitational field. As for the Doppler effect, its importance depends on the magnitude of the pulsar's velocity projected on to the line of sight. Consequently, different measurements are sensitive to different orbital parameters.

For example the Roemer delay is sensitive to the (projected) size of the orbit. Two orbits of the same projected size but with slightly different velocities will be indistinguishable from the point of view of the Roemer delay. The Einstein delay depends on the variation of the gravitational potential (i.e. m_2/r) from the companion star. Roughly speaking, this effect depends on the eccentricity and semimajor axis of the orbit. Hence, two orbits with the same eccentricity and same semimajor axes will be considered as nearly identical orbits if only the Einstein time delay is used to determine the binary parameters. The Doppler effect depends on the projected velocity and is therefore not as sensitive to the shape of the orbit.

In practice, all of these different time delays are combined to estimate the best-fitting orbital parameters. Whether two orbits are distinguishable or not depends on the binary parameters, the orientation of the orbit, and the noise level, which introduce random factors into the estimated parameters. A detailed and observationally consistent definition of 'nearly identical' orbits is complex and is beyond the scope of this work. In the following, we will use a few

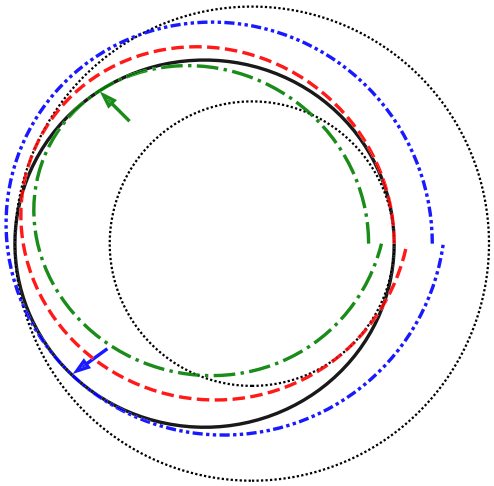

Figure 3. This is a representation of different definitions of nearly identical perturbed orbits. The solid ellipse represents the unperturbed orbit. The two dotted circles represent circular orbits with radii $r_{\rm min}$ and $r_{\rm max}$. The semi-ellipses represent perturbed orbits which are nearly identical to the ellipse under different definitions. The dashed semi-ellipse represents a perturbed orbit with the same $r_{\rm min}$ and $r_{\rm max}$ as the unperturbed orbit. The dashed–dotted semi-ellipse and the dashed–dotted–dotted semi-ellipse represent an orbit that connects to the unperturbed orbit smoothly at $\phi = 0.75\pi$ and $\phi = 1.2\pi$, respectively. Each of the connecting points is highlighted with an arrow. The perturbation is exaggerated (i.e. $\epsilon \sim 0.15$) to assist visualization.

simplified assumptions to demonstrate how the definition of nearly identical orbits affects the value of the GM clock effect. We will consider a few typical examples which are presented in Fig. 3.

A system dominated by the Einstein delay would consider orbits with the same $r_{\rm min}$ and $r_{\rm max}$ as nearly identical. Because $r = \sqrt{\rho^2 + z^2}$, the oscillation in the z -direction only contributes to changes in the radial distance at second order in ϵ. Therefore, we have $r_{\rm min} \approx \rho_{\rm min} = u_{\rm max}$ and similarly for $r_{\rm max}$. This requires

$$\alpha = \frac{C_2(1+{e_0}^2)}{1-{e_0}^2}\,, \tag{29}$$

$$\eta = C_2\,. \tag{30}$$

Using this relation in the case of $\Delta\mathcal{T}_{\rm orb} = 0$ (i.e. the anomalistic period), the clock effect between the period of the perturbed and that of the unperturbed orbit is given by

$$\begin{aligned}\Delta\mathcal{T}_{\rm size} + \Delta\mathcal{T}_{\rm fixed} &= -\frac{\pi\left(C_\rho - 2C_\phi\right)}{M\sqrt{1-{e_0}^2}} \\ &= \frac{3\pi\left[(k-2)\sigma\cos\theta_\sigma - 2S\cos\theta_S\right]}{M\sqrt{1-{e_0}^2}}\,.\end{aligned} \tag{31}$$

Since the coefficients of σ and S are both negative (for $k = 0$, 1/2, 1), this implies that when $\Delta\mathcal{T}_{\rm orb} = 0$, it takes less time for a binary to complete a full revolution on a prograde orbit than on an unperturbed orbit or a perturbed retrograde orbit. This counter-intuitive conclusion is specific to the anomalistic period. As spin–orbit coupling forces cause the orbit to precess, the periaspsis vectors rotate in the opposite direction of the angular velocity for prograde orbits. Therefore, an anomalistic period is complete for $\Delta\phi < 2\pi$ on a prograde orbit, so that the time it takes to finish a full revolution is in fact shorter than the corresponding unperturbed or retrograde orbit.

Another example is given by a system that connects the perturbed orbit and unperturbed orbit smoothly. If we assume the unperturbed orbit turns into a perturbed orbit at $\phi = \phi_0$, it is equivalent to assuming that the spin–orbit coupling force is turned on at $\phi = \phi_0$. We require that u, $\dot{u}$, and $\dot{\phi}$ of the perturbed orbit at $\phi = \phi_0$ coincide with their counterparts of the unperturbed orbit. Similarly, we have $z = \dot{z} = 0$ at $\phi = \phi_0$. This requires

$$\begin{aligned}\alpha = \;& \frac{a_0 M^2}{6{L_0}^5}\{2e_0(C_\rho + C_\phi)[2{e_0}^2\cos^3(\phi_0 - \omega_0) \\ &+ 3e_0\cos(2\phi_0 - 2\omega_0) + 6\cos(\phi_0 - \omega_0)] \\ &+ 3({e_0}^4 + {e_0}^2 + 2)C_\rho - 3({e_0}^2 - 5){e_0}^2 C_\phi\}\,.\end{aligned} \tag{32}$$

We omit the formula of the GM clock effect under this condition as it is redundant.

4 COMPARISON WITH PREVIOUS STUDIES

In this section, we compare the GM clock effect we defined with the results from Mashhoon et al. (2001), Bini et al. (2004a,b), Mashhoon & Singh (2006), and Hackmann & Lämmerzahl (2014). The systems they studied are all extreme-mass-ratio-inspiral (EMRI) systems, with special focus on the Earth-satellite system. For an EMRI system, we consider m_1 to be the mass of the test particle and m_2 to be the massive object. This system could refer to a pulsar orbiting a massive black hole or a satellite orbiting the Earth. Therefore, we have $m_1/m_2 \ll 1$ and $M \equiv m_1 + m_2 \approx m_2$. To leading order in the mass ratio, we have $\boldsymbol{S} \approx \boldsymbol{S}_2 \sim m_2^2$ and $\boldsymbol{\sigma} = m_2\boldsymbol{S}_1/m_1 + m_1\boldsymbol{S}_2/m_2 \sim m_1 m_2$. We note that for the Earth-satellite system $\boldsymbol{\sigma} = 0$ due to the negligible spin of the satellite. Furthermore, we note that in Bini et al. (2004a,b)and Mashhoon & Singh (2006), they have used $\boldsymbol{\sigma} = m_2\boldsymbol{S}_1/m_1$ instead, such that the clock effect formula is accurate to leading order in mass ratio for $\boldsymbol{S}_1$ and $\boldsymbol{S}_2$, respectively.

In addition, the EOMs for the test particles are usually described as geodesics (with or without perturbations due to the spin of the small mass $\boldsymbol{S}_1$) in the Kerr space–time, and the inertial frame is usually defined with reference to $\boldsymbol{S}_2$, instead of the orbital angular momentum. The observer's frame $(x',\ y',\ z')$ is defined such that $\boldsymbol{S}$ overlaps with the z'-axis. Therefore, the inclination angle of the orbital plane ι is equivalent to θ_S. This difference in definition encodes implicit restrictions of the parameter space and naturally leads to discrepancies in the results, as illustrated in the following sections.

4.1 Mashhoon's clock effect

Mashhoon et al. (2001) investigated the clock effect of a test particle orbiting the Earth. The mass and spin of the Earth dominates the spin–orbit coupling forces. Therefore, the mass–weighted spin vector $\boldsymbol{\sigma}$ and the spin $\boldsymbol{S}_1$ can be ignored. For the observer on the Earth, its z' axis matches the spin axis, i.e. $\theta_S = \iota$ and $\phi_S = \pi/2$. The two degrees of freedom in the $H(\phi)$ are removed by requiring $H(\phi_0) = H'(\phi_0) = 0$. With these conditions, the coefficients of the forces are given by

$$C_\rho = 2S\cos\iota\,, \tag{33a}$$

$$C_\phi = -2S\cos\iota\,, \tag{33b}$$

$$C_{z,\rho} = 2S\cos\phi\sin\iota\,, \tag{33c}$$

$$C_{z,\phi} = 4S\sin\phi\sin\iota\,. \tag{33d}$$

These conditions yield $C_2 = 0$, where the orbital semimajor axis and eccentricity of the perturbed orbit coincide with a and e. The authors

defined a full orbit using the sidereal period, i.e. equation (25). This is equivalent to fixing the angle ϕ_1 to be

$$\phi_1 = -\frac{4\pi M}{{L_0}^3} S \sin\iota \tan\iota \cos^2\phi_0 \,. \tag{34}$$

Mashhoon et al. (2001) commented that ι should not be near $\pi/2$ to ensure ϕ_1 remains small, given the divergence of $\tan\iota$ around $\iota = \pi/2$. We seek to provide a more precise range of the required inclination angle. For a satellite in low Earth orbit, to ensure that $\phi_1 \ll 1$, we must have

$$\begin{aligned}\frac{\pi}{2} - \iota &\gg \frac{4\pi M_\oplus I_\oplus \omega_\oplus}{(aM_\oplus)^{3/2}} \\ &= 1.7\times10^{-10}\,\mathrm{rad}\left(\frac{I_\oplus}{8\times10^{37}\,\mathrm{kg\,m^2}}\right)\left(\frac{6400\,\mathrm{km}}{a}\right)^{3/2},\end{aligned} \tag{35}$$

where we have used $I_\oplus \simeq 0.33 M_\oplus {R_\oplus}^2$ to calculate the Earth's moment of inertia, with the coefficient 0.33 taken from Williams (1994). This condition implies that equation (34) remains valid for the majority of existing satellites, suggesting that the clock effect could potentially be revealed with existing data. The time it takes to complete an azimuthal closure is therefore

$$\mathcal{T} = 2\pi\sqrt{\frac{a^3}{M}} + \frac{2\pi S\cos\iota}{M}\left\{\frac{4 - 2\cos^2\phi_0\tan^2\iota}{\left[1+e\cos(\phi_0-\omega)\right]^2} - \frac{3}{\sqrt{1-e^2}}\right\}. \tag{36}$$

This result agrees precisely with equation (30) of Mashhoon et al. (2001).

4.2 Bini's results: circular equatorial orbits with spinning secondary

Bini et al. (2004a,b) studied the GM clock effects in EMRIs with both perturbed and unperturbed orbits, which are strictly circular and restricted to the equatorial plane. The unperturbed orbit, the perturbed prograde orbit, and the perturbed retrograde orbit, are all assumed to have the same radius. This corresponds to cases with $e = e_0 = 0$ and $\alpha = 0$, such that $a = a_0$ represents the constant distance between the binary pair. Both spins are required to be perpendicular to the orbital plane (i.e. $\sin\theta_\sigma = \sin\theta_S = 0$) such that the motion in the z-direction vanishes. For a strictly circular orbit, we have $\phi_1 = 0$ regardless of the orientation of the observer's plane. The time it takes for the binary to complete one orbit becomes

$$\mathcal{T} = 2\pi\sqrt{\frac{a^3}{M}} + \frac{2\pi}{M}\left(\pm\frac{3}{2}k\sigma \pm S\right), \tag{37}$$

where the plus (minus) sign depends on the relative orientation of the spin axis and corresponds to the spin axis being aligned (anti-aligned) with the orbital angular momentum. For an EMRI system, assuming $\boldsymbol{\sigma} \simeq m_2\boldsymbol{S}_1/m_1$ and $\boldsymbol{S} \simeq \boldsymbol{S}_2$, the orbital time-scale becomes

$$\mathcal{T} = 2\pi\sqrt{\frac{a^3}{M}} + \frac{2\pi}{M}\left(\pm\frac{3}{2}k\frac{M}{m_1}S_1 \pm S_2\right). \tag{38}$$

This result matches equations (3.2) and (3.3) of Bini et al. (2004b) for the three SSCs considered in their paper. It also matches the result of Faruque (2004) when $k = 1$.

4.3 Mashhoon and Singh's results

Mashhoon & Singh (2006) studied the GM clock effect for an EMRI system on a semicircular orbit close to the equatorial plane. The circular geodesics are considered as unperturbed orbits and the force due to the interaction of curvature with the spin of the test particle ($\boldsymbol{S}_1$) is considered as the perturbing force. The spin of the massive object is therefore either aligned or anti-aligned with the orbital angular momentum, but there is no restriction on the orientation of the smaller spin.

The nearly identical perturbed orbit is defined as the orbit that the test particle will follow if the force due to the smaller spin is switched on at $t = 0$. More specifically, two orbits with the same $\boldsymbol{S}$ but with either vanishing $\boldsymbol{S}_1$ or non-vanishing $\boldsymbol{S}_1$, that share the same u, $\dot{u}$, ϕ, $\dot{\phi}$, and $z = 0 = \dot{z}$ at $t = 0$, are considered nearly identical. The azimuthal closure is defined as $\phi_0 \to \phi_0 + 2\pi$, such that the motion in the z-direction (and hence the projection of the spin on to the orbital plane) can be ignored and we have $\phi_1 = 0$. Under this condition, we have $e_0 = 0$ and

$$\alpha = e_0\eta = \frac{3k\sigma}{\sqrt{{a_0}^3 M}}. \tag{39}$$

The unperturbed orbit is strictly circular but the perturbed orbit admits a small eccentricity. The time it takes for the smaller particle to complete one full orbit is

$$\mathcal{T} = 2\pi\sqrt{\frac{{a_0}^3}{M}} + \frac{2\pi}{M}\left(6k\frac{M}{m_1}S_1\cos\theta_{S_1} \pm S_2\right). \tag{40}$$

The sign in front of S_2 depends on the relative orientation of the orbit. As the perturbed orbit remains close to the equatorial plane, the sign of S_2 is positive (negative) when the spin of the black hole is aligned (anti-aligned) with the orbital angular momentum. The angle θ_{S_1} is not restricted and can be written as $\hat{\boldsymbol{S}}_1 \cdot \hat{\boldsymbol{J}}$. Mashhoon & Singh (2006) used the Tulczyjew–Dixon condition, which suggests $k = 1$. Under this condition, our result becomes equivalent to equation (57) in their paper. In comparison to the work of Bini et al. (2004a,b) and Faruque (2006), the coefficient of S_1 in Mashhoon & Singh (2006) and equation (40) is much larger. We confirm that the difference in this coefficient is merely an artefact of the different literature definitions of 'nearly identical' orbits.

4.4 Hackmann and Lämmerzahl's results

Hackmann & Lämmerzahl (2014) compared inclined orbits of a non-spinning test particle in the Kerr and Schwarzschild space–times. The Kerr geodesics were considered to be the perturbed orbit while the Schwarzschild geodesics were the unperturbed orbit. The spin axis $\boldsymbol{S} = \boldsymbol{S}_2$ was aligned (or anti-aligned) with the z-axis, while the orbital angular momentum was inclined at an angle ι with respect to the z-axis. The orbit precesses and nutates at different frequencies around the spin axis, as a consequence of the spin–orbit coupling force. They calculated the clock effect by averaging the azimuthal velocity over radial oscillation and altitudinal oscillation, respectively. As these two oscillations have different frequencies in the presence of perturbative forces, their result is equivalent to averaging the GM clock effect over infinite time. Further, by using the inverse azimuthal velocity to derive the clock effect, they have effectively considered the azimuthal closure condition and their formula represents the infinitely averaged sidereal period. Consequently, their result is independent of the argument of periapsis of the orbit. The formula, i.e. equation (30) of Hackmann & Lämmerzahl (2014), in our notation reads:

$$\Delta\mathcal{T} = \frac{2\pi S}{M}\frac{\left(3e^2+2e+3\right)\cos\iota - 2e - 2}{\left(1-e^2\right)^{3/2}}. \tag{41}$$

In general, spin–orbit coupling forces give rise to the GM clock terms that contain θ_S (which is equivalent to ι in this case). However, their formula has a component that is independent of ι. We argue that this term is a direct consequence of the precession of the orbital angular momentum and that, although not explicitly stated, their averaging method has assumed the orbital angular momentum of the non-spinning test particle to be much smaller than $\boldsymbol{S}$. When $S \gg \mu L$, the orbital angular momentum approximately precesses around the spin axis (Kidder 1995) with

$$\dot{\boldsymbol{L}} = \frac{2}{r^3}\, \boldsymbol{S}_2 \times \boldsymbol{L}\,. \tag{42}$$

The prograde motion acquires a positive angular velocity such that $\omega_S = 2S_2/r^3$, regardless of the inclination angle. In fact, this angular velocity is the precession speed of the longitude of the ascending node (i.e. nodal precession) of the satellite (Lense & Thirring 1918). The correction to the orbital period due to this angular velocity is

$$\Delta\mathcal{T} = \frac{2\pi}{\omega_{\rm N}+\omega_S} - \frac{2\pi}{\omega_{\rm N}} = -\frac{4\pi S}{M} + \mathcal{O}(S^2)\,, \tag{43}$$

for a circular orbit, which is equivalent to the part of equation (41) that is independent of the inclination angle when $e = 0$. Here,$\omega_{\rm N} = \sqrt{M/r^3}$ is the Newtonian angular velocity. This relation implies that the inclination-independent component of the clock effect originates from the nodal precession of the orbit. During the node's prograde precession with respect to the spin of the massive object, it contributes to reducing the orbital period of the prograde motion and increasing the orbital period of the retrograde motion. As the azimuthal velocity has been averaged over infinite time, the clock effect was calculated with respect to a distant and fixed observer located on the $x' - y'$ plane. This physical picture suggests that the spinning axis is effectively fixed with respect to the distant observer while the orbital angular momentum precesses about this axis. As both spin and orbital angular momenta precess around the total angular momentum, $\boldsymbol{J} = \boldsymbol{S}_2 + \mu\boldsymbol{L}$, this picture is only valid when $\boldsymbol{J} \approx \boldsymbol{S}_2$, which implies $|\boldsymbol{S}_2| \gg \mu|\boldsymbol{L}|$. This requirement suggests that the formula will be valid in the test particle limit (e.g. an Earth-satellite system) but may be violated in compact pulsar-black hole systems, where the angular momentum of the pulsar is non-negligible compared with the black hole's spin.

In comparison, our perturbation method is valid regardless of the mass ratio and whichever angular momentum dominates. Since we have ignored precession of the orbital angular momentum and spin angular momenta, our formula is valid when the observational time-scale is much shorter than the precession time-scale. For this reason, it is unnecessary to compare our formula with the result of Hackmann & Lämmerzahl (2014). Nevertheless, these two methods lead to consistent results when the spin axes are approximately aligned (or anti-aligned) with orbital angular momentum, as precession may be ignored in such cases. When $\iota = 0$, equation (36) reduces to

$$\begin{aligned}\Delta\mathcal{T} &= \frac{2\pi S}{M}\left\langle -\frac{3}{\sqrt{1-e^2}} + \frac{4}{\left[1+e\cos(\phi_0-\omega)\right]^2}\right\rangle_{\omega} \\ &= \frac{2\pi S}{M}\,\frac{1+3e^2}{\left(1-e^2\right)^{3/2}}\,,\end{aligned} \tag{44}$$

where $<\cdots>_{\omega}$ represents averaging over ω. This is the same as equation (41) for $\iota = 0$.

4.5 Further comments on the clock effect

It has been shown that the differences in various results in the literature are due to the choice of SSC (i.e. the value of k), the definition of 'nearly identical' orbits (i.e. the value of α), and the definition of a full revolution (i.e. the value of ϕ_1). For example the constant coefficients in front of the secondary spin could differ by a factor of four in equations (38) and (40), even for the same SSC, as a consequence of different definitions of 'nearly identical' orbits. In fact, the coefficients can be made arbitrarily large or small with suitable choices of α and ϕ_1. Some coefficients appear in the literature more often than others, simply because their underlying definitions seem more natural for the system being considered, as compared with others.

We seek to further illustrate this effect by showing that even the well-known formula equation (1) admits variants. Consider an Earth-satellite system with a satellite moving on an unperturbed circular orbit on the equatorial plane of the Earth. We now define a nearly identical perturbed orbit as one that connects to the circular unperturbed orbit smoothly at periapsis. For an unperturbed orbit with radius a_0, we then have

$$\alpha = \frac{C_\rho}{{a_0}^{3/2} M^{1/2}}\,. \tag{45}$$

The GM clock effect is now given by

$$\mathcal{T}_+ - \mathcal{T}_- = \frac{16\pi S}{M}\,. \tag{46}$$

To the best of our knowledge, only the constant coefficient 4π appears in the literature. This is because it seems more natural to consider two orbits with the same size ($r_{\rm min}$ and $r_{\rm max}$) as being nearly identical. For pulsar timing, this is indeed the case as the Roemer delay is, in general, the dominant time delay (with order $\sim r/c$), while the other effects depend on v/c (the Doppler effect), $(v/c)^2$ (the Einstein delay), or Gm_2/c^3 (the Shapiro delay). However, the Roemer delay is only sensitive to the projected size of the orbit, hence for binaries with nearly face-on orientations the Roemer delay will vanish and decoding other time delays will be necessary to acquire the full information of the orbital parameters in pulsar timing observations.

5 CONCLUSIONS

In this study, we have derived the GM clock effects for a binary system with arbitrary mass ratio, eccentricity, inclination angle, and spin orientation. The difference in orbital period between a spinning binary and a non-spinning binary is given by equation (22). The generic clock effect admits three degrees of freedom: the choice of SSC (i.e. value of k) which comes from the dependence of spin–orbit coupling forces on the SSC, the definition of 'nearly identical' orbits (i.e. the value of α), and the definition of a full revolution (i.e. the value of ϕ_1). We demonstrate how these various definitions of 'nearly identical' orbits affect the clock effect in Section 3.5 and show how the definition of a full revolution affects the clock effect in Section 3.4.

When the spin–orbit force is present, the orbit can no longer to be identical to orbits where the spin–orbit coupling force is absent. This can also be explained by the fact that the spin is non-degenerate and cannot be mimicked by a Newtonian non-spinning binary. Therefore, the GM clock effects depend on the orbits being compared. We refer to those orbits being compared as 'nearly identical' orbits and argue that this definition should be observationally motivated. In Section 3.5, we presented some examples of possible definitions of 'nearly identical' orbits that are

relevant for pulsar timing observations and demonstrated that these would lead to different formulae for the GM clock effects.

In the context of general relativity, the definition of a full revolution is not unique, unlike in Newtonian mechanics. This is due to the precession of the argument of periapsis, which gives rise to at least two different definitions: the sidereal period and the anomalistic period. For nearly edge-on orbits, the sidereal period corresponds to the time interval between two total eclipses (or two successive maxima of the Shapiro delay). For nearly face-on orbits, the anomalistic period is a more sensible definition, as it represents the time interval between successive maxima of the Einstein delay. It is also possible to define the orbital period as the nodal period, but the physical meaning of this definition is ambiguous. For binaries with an intermediate inclination angle, finding a sensible definition is complicated by the potential degeneracy between the orbital parameters.

We compare the existing expressions in the literature (in Section 4) and demonstrate that the generic clock effect formula that we derive can recover most of these results. We have identified the source of discrepancies in the literature and explained these differences using the three degrees of freedom mentioned earlier. Compared to previous works, our generic clock effect formula can be applied to a broader parameter space, including, but not limited to, extreme-mass-ratio binaries. This study thus provides a useful framework for the investigation of GM clocks effects and orbital dynamics in a broad range of systems, from artificial satellites around the Earth to general astrophysical systems containing two spinning compact objects in close orbits around each other.

ACKNOWLEDGEMENTS

We are grateful to Prof Bahram Mashhoon for valuable in-depth discussions on gravito-electromagnetism analogy and the associated gauge issues. Kaye JL was supported by a PhD Scholarship from the Vinson and Cissy Chu Foundation, and by a University College London Mathematical & Physical Sciences (MAPS) Dean's Prize. Ziri Y was supported by a United Kingdom Research and Innovation (UKRI) Stephen Hawking Fellowship. Joana T was supported by a United Kingdom Science and Technology Facilities Council (UK STFC) Research Studentship. Kinwah W and Joana T acknowledge support from the University College London Cosmoparticle Initiative. This work was supported in part by a United Kingdom Science and Technology Facilities Council (UK STFC) Consolidated Grant awarded to University College London Mullard Space Science Laboratory. This research has made use of NASA's Astrophysics Data System (ADS), MATHEMATICA, and the MATPLOTLIB package.

DATA AVAILABILITY

No new data were generated or analysed in support of this research.

REFERENCES

Aharonov Y., Bohm D., 1959, Phys. Rev., 115, 485
Archibald A. M. et al., 2018, Nature, 559, 73
Barausse E., Racine E., Buonanno A., 2009, Phys. Rev. D, 80, 104025
Barker B. M., Oconnell R. F., 1979, Gen. Relat. Gravit., 11, 149
Bini D., Jantzen R. T., Mashhoon B., 2001, Class. Quant. Grav., 18, 653
Bini D., Jantzen R. T., Mashhoon B., 2002, Class. Quant. Grav., 19, 17
Bini D., de Felice F., Geralico A., 2004a, Class. Quant. Grav., 21, 5427
Bini D., de Felice F., Geralico A., 2004b, Class. Quant. Grav., 21, 5441
Braginskii V. B., Caves C. M., Thorne K. S., 1977, Phys. Rev. D, 15, 2047
Clark S. J., Tucker R. W., 2000, Class. Quant. Grav., 17, 4125
Cohen J. M., Mashhoon B., 1993, Phys. Lett. A, 181, 353
Cohen J. M., Rosenblum A., Clifton Y., 1988, Phys. Lett. A, 131, 163
Corinaldesi E., Papapetrou A., 1951, Proc. R. Soc. Lond. Ser. A, 209, 259
Costa L. F., Herdeiro C., Natário J., Zilhão M., 2012, Phys. Rev. D, 85, 024001
Dixon W. G., 1964, Il Nuovo Cimento, 34, 317
Edwards R. T., Hobbs G. B., Manchester R. N., 2006, MNRAS, 372, 1549
Faruque S. B., 2004, Phys. Lett. A, 327, 95
Faruque S. B., 2006, Phys. Lett. A, 359, 252
Faruque S. B., Ahsan M. H., Ishwar B., 2003, Phys. Lett. A, 312, 166
Frenkel J., 1926, Z. Phys., 37, 243
Gronwald F., Gruber E., Lichtenegger H., Puntigam R. A., 1997, preprint(gr-qc/9712054)
Hackmann E., Lämmerzahl C., 2014, Phys. Rev. D, 90, 044059
Hanson A. J., Regge T., 1974, Ann. Phys., 87, 498
Harris E. G., 1991, Am. J. Phys., 59, 421
Iorio L., Mashhoon B., 2024, Ann. Phys. (Berlin), 536, 2300466
Iorio L., Lichtenegger H., Mashhoon B., 2002, Class. Quant. Grav., 19, 39
Kerr A. W., Hauck J. C., Mashhoon B., 2003, Class. Quant. Grav., 20, 2727
Kidder L. E., 1995, Phys. Rev. D, 52, 821
Kimpson T., Wu K., Zane S., 2019, MNRAS, 486, 360
Kimpson T., Wu K., Zane S., 2020, MNRAS, 497, 5421
Lense J., Thirring H., 1918, Phys. Z., 19, 156
Li K. J., Wu K., Singh D., 2019, MNRAS, 485, 1053
Li K. J., Wu K., Leung P. K., Singh D., 2022, MNRAS, 511, 3602
Lichtenegger H. I. M., Gronwald F., Mashhoon B., 2000, Advances in Space Research, 25, 1255
Lorimer D. R., 2008, Living Rev. Relativ., 11, 8
Lorimer D. R., Kramer M., 2012, Handbook of Pulsar Astronomy. Cambridge Univ. Press, Cambridge
Loutrel N., Liebersbach S., Yunes N., Cornish N., 2019, Class. Quant. Grav., 36, 025004
Manchester R. N., 2017, J. Astrophys. Astron., 38, 42
Mann A., 2018, Proc. Natl. Acad. Sci., 115, 7449
Mashhoon B., 1978, ApJ, 223, 285
Mashhoon B., 2001, in Pascual-Sánchez J. F., Floría L., San Miguel A., Vicente F., eds, Reference Frames and Gravitomagnetism. World Scientific Publishing, Singapore
Mashhoon B., 2007, The Measurement of Gravitomagnetism: A Challenging Enterprise. Nova Science, New York, USA, 29–39
Mashhoon B., Singh D., 2006, Phys. Rev. D, 74, 124006
Mashhoon B., Gronwald F., Theiss D. S., 1999, Ann. Phys., 8, 135
Mashhoon B., Iorio L., Lichtenegger H., 2001, Phys. Lett. A, 292, 49
Mathisson M., 1937, Acta Phys. Pol., 6, 163
Newton T. D., Wigner E. P., 1949, Rev. Mod. Phys., 21, 400
Overstreet C., Asenbaum P., Curti J., Kim M., Kasevich M. A., 2022, Science, 375, 226
Pryce M. H. L., 1948, Proc. R. Soc. Lond. Ser. A, 195, 62
Remmen G. N., Wu K., 2013, MNRAS, 430, 1940
Shao L., 2016, Phys. Rev. D, 93, 084023
Singh D., Wu K., Sarty G. E., 2014, MNRAS, 441, 800
Stairs I. H., 2003, Living Rev. Relativ., 6, 5
Tartaglia A., 2000, Gen. Relat. Gravit., 32, 1745
Taylor J. H., Weisberg J. M., 1989, ApJ, 345, 434
Teyssandier P., 1977, Phys. Rev. D, 16, 946
Teyssandier P., 1978, Phys. Rev. D, 18, 1037
Thorne K. S., 1988, in Fairbank J. D., Deaver B. S. J., Everitt C. W. F., Michelson P. F., eds, Near Zero: New Frontiers of Physics. p. 573 W. H. Freeman and Company, New York, USA
Tulczyjew W., 1959, Acta Phys. Pol., 18, 931
Vladimirov I. S., Mitskevich N. V., Horsky J., 1984, Space, time, and gravitation. Mir Publishers Moscow
Voisin G., Cognard I., Freire P. C. C., Wex N., Guillemot L., Desvignes G., Kramer M., Theureau G., 2020, A&A, 638, A24
Weisberg J. M., Taylor J. H., 2005, in Rasio F. A., Stairs I. H., eds, ASP Conf. Ser., Vol. 328, Binary Radio Pulsars. Astron. Soc. Pac., San Francisco, p. 25
Williams J. G., 1994, AJ, 108, 711
Wu K., 2022, Universe, 8, 78

APPENDIX A: EQUATION OF MOTION AND GAUGE SYMMETRY

The GM clock effect is a consequence of the analogy between electromagnetic and gravitational field. It was initially derived (e.g. Vladimirov, Mitskevich & Horsky 1984; Mashhoon et al. 2001; Iorio et al. 2002) from a Lorentz-force-like formula, with the gravito-electric field arising from the point mass, and the GM (gravito-magnetic) field taking the form of a magnetic dipole (see e.g. Braginskii, Caves & Thorne 1977; Thorne 1988; Harris 1991; Clark & Tucker 2000; Mashhoon 2001, 2003; Iorio & Mashhoon 2023). In this work, we adopt the spin–orbit coupling representation, similar to that in Barker & Oconnell (1979) through equation (2), an approach different from the approaches that explicitly use the Lorentz-force-like formula. The difference in the two formula stems from the geometrical nature of gravity. While gauge transformation does not interfere with the coordinates in the electromagnetic theory, gauge transformation explicitly changes the coordinates in general relativity, and the Lorentz-force-like formula appears a specific gauge choice, commonly referred to as the (gravito-electromagnetic) GEM gauge. Consequently, there is some arbitrariness in the definition of the GM field, depending on the construction of the analogy and the adopted gauge-fixing conditions (see e.g. Clark & Tucker 2000; Mashhoon 2001). Owning to this subtlety, it is unsurprising that the spin–orbit coupling force presented in this work, which is derived under the standard pN gauge and ADM gauge, differs from that of the GEM gauge. These disparities can be reconciled through appropriate coordinate transformations. However, we are not aware of existing literature that addresses this difference, possibly due to the limited overlap between the two fields. Since Newtonian gravity does not exhibit this subtlety, the differences between these sets of coordinates become apparent, at least at the 1pN order.

The intricacies of this coordinate issue become particularly relevant when connecting a locally defined field (e.g. the GM field) with a globally defined concept (e.g. orbital size and eccentricity), which are commonly employed in pulsar timing, satellite ranging, and similar observations. To counter this ambiguity, gauge-invariant quantities like orbital frequency and Detweiler's redshift have been widely adopted to avoid coordinate-dependent artefacts. It's important to note that classical GM clock effect, as demonstrated in equation (1), does not exhibit such coordinate-dependent artefacts, owing to its topological characteristics and symmetrical nature. Despite variations arising from different schemes, the same clock difference is consistently obtained without the need to clarify the difference in coordinates.

Aligning two artificial satellites in the exact opposite yet the same orbit is a challenging task. Realistic measurements need to account for formulae that incorporate orbital size and eccentricity information, which, inevitably, are written in a coordinate-dependent manner. The appearance of eccentricity may raise concerns, especially given the various different definitions of eccentricity (see e.g. Loutrel et al. 2019), and the unconventional definition we have adopted. As the clock effect due to eccentricity is already a perturbation at the 1.5pN level, any alternative definition of eccentricity would alter the clock effect at (at least) the 2.5pN order. Therefore, we can safely ignore when considering leading-order effects.

In contrast, the semimajor axis presents a more serious challenge, as discussed earlier. We attempt to address this by introducing the somewhat arbitrary parameter α in equation (23a). Exploring the intricate differences in coordinates defined in various gauges is beyond the scope of this work. Instead, our focus is on directing the audience's attention to the observationally oriented definitions, as argued in Sections 3.4 and 3.5.

This paper has been typeset from a TEX/LATEX file prepared by the author.